Available online at www.sciencedirect.com

ScienceDirect

Advances in Space Research 69 (2022) 26–34

ADVANCES IN SPACE RESEARCH (a COSPAR publication)

www.elsevier.com/locate/asr

Seismo-ionospheric anomalies before the 2019 Mirpur earthquake from ionosonde measurements

Junaid Ahmed [a,*], Munawar Shah [b,c], Muhammad Awais [a], Shuanggen Jin [d], Waqar Ali Zafar [a], Nabeel Ahmad [a], Ayaz Amin [e], Muhammad Ali Shah [a], Ikram Ali [f]

[a] Centre for Earthquake Studies, National Centre for Physics, Islamabad, Pakistan
[b] Institute of Space Technology, Islamabad, Pakistan
[c] Department of Space Science, GNSS and Space Education Research Lab, National Center for GIS and Space Applications, Institute of Space Technology, Islamabad, Pakistan
[d] Shanghai Astronomical Observatory, Chinese Academy of Sciences, Shanghai 200030, China
[e] Space Weather Monitoring Division, SUPARCO, Karachi, Pakistan
[f] Exploration Department, KPOGCL, Pakhtunkhwa, Pakistan

Received 9 October 2020; received in revised form 9 June 2021; accepted 26 July 2021
Available online 2 August 2021

Abstract

The rapid advancement in ground and space based ionospheric measurements provide an opportunity to work on different earthquake precursors for lithosphere-ionosphere coupling hypothesis. In this paper, the peak plasma ionospheric frequency (f_oF2) for 90 days before/after the main shock of September 24, 2019 (M5.6) earthquake in Pakistan are studied for earthquake precursors from ionosonde stations located at Islamabad and Sonmiani. We implement the 30 days running median technique to detect the abnormality in f_oF2 over the epicenter of impending earthquake. A comprehensive analysis of these anomalies on two stations is performed in order to extract the maximum of these abnormalities in their respective regions. The deviation in hourly data in Sonmiani station shows significant variation within 10–20 days before the main shock, as most of the values within 5–10 days' window are within the confidence limits. On the other hand, positive and negative deviations in the analysis of Islamabad station may be revealed as a possible signature of seismo-ionospheric anomalies. The major reason of these seismo-ionospheric anomalies is the distance between the ionosonde station and epicenter, where Islamabad station is close to the epicenter as compared to Sonmiani. It is noteworthy that both negative and positive deviations are observed before the M5.6 earthquake; however, the intensity of positive anomalies is more than negative anomalies. Moreover, severe positive deviation occurs within 10–20 days before the earthquake at the Sonmiani station. Also, there is no geomagnetic storm within 10 days before the earthquake which opposes the existence of seismo-ionospheric anomalies. The evidence supports that these seismo-ionospheric precursors are probably due to the lithospheric-ionospheric coupling.
© 2021 COSPAR. Published by Elsevier B.V. All rights reserved.

Keywords: Lithospheric-ionospheric coupling; Ionospheric frequency (f_oF2); Seismo-ionospheric anomalies; Median technique; Epicenter; Ionosonde

1. Introduction

There are many reports about the possible coupling of seismo-ionospheric anomalies before large earthquakes from different ground and satellite measurements (e.g., Pulinets et al., 2003; Shah and Jin, 2015; Ahmed et al., 2018; Akhoondzadeh et al., 2019; Marchetti et al., 2020;

* Corresponding author at: Centre for Earthquake Studies, NCP Complex, Shahdra Valley Road, Islamabad, Pakistan.
E-mail address: junaid.ahmed@ncp.edu.pk (J. Ahmed).

https://doi.org/10.1016/j.asr.2021.07.030
0273-1177/© 2021 COSPAR. Published by Elsevier B.V. All rights reserved.

Shah et al., 2021). Nevertheless, the technique of detecting these ionospheric anomalies vary from one earthquake to another due to seasonal variations in ionosphere, which cause complication in the earthquake preparation zone (Marchetti et al., 2020a,b; Rishbeth, 2006; Rishbeth et al., 2009; Shah et al., 2019b). Most of the studies report ionospheric anomalies within 5–10 days before and after the main shock of different earthquakes in seismogenic zone (Shah et al., 2020a,b,c). For example, Shah and Jin (2018) investigated the long-term ionosphere data over the earthquake preparation zones and showed positive and negative anomalies within 5–10 days associated with main shock. Furthermore, they showed that ionospheric anomalies are related with earthquakes of M > 6.0 and shallow hypocentral depths.

There are different methods for the detection of ionospheric anomalies before and after the main shock in earthquake preparation period. These anomalies have been categorized to be either positive or negative in a specific day corresponding to the background data. The anomaly beyond upper confidence bounds can be positive and similarly low-level anomaly than lower confidence bound is negative anomaly (Liu et al., 2006). Various anomalous ionospheric perturbations are used for the detection of these anomalies; e.g., the method of standard deviations by Le et al. (2011), the 1.5 times lower and upper quartiles by Liu et al. (2006), the semi inter quartile range (Liu et al., 2006), the method of interquartile range (Liu et al., 2004). However, some reports show that these anomalies may rise up to 35 days before an earthquake (Perrone et al., 2010). A recent mega thrust off the east coast of Honshu, Japan on March 11, 2011 reported significant deviation in the data of Total Electron Content from Global Positioning System (GPS TEC) – approximately 40 min before this event (Heki, 2011). Some reports showed three different sources of ionospheric perturbations: 1st is the solar flare activity from the sun, 2nd is the geomagnetic variations due to the earth magnetic field and 3rd is the meteorological effects due to weather changes (e.g., Hajkowicz 1991; Forbes et al., 2000; Rishbeth and Mendillo, 2001; Mendillo et al., 2002; Rishbeth, 2006; Shahzad et al., 2021). The geomagnetic storms and solar activity give rise to an extensive electron density depletions or enhancements, also donated as positive and negative storm, respectively (Mendillo, 2006), which is more than the variations caused of ionospheric variations of an earthquake.

The seismo-ionospheric anomalies are explained by two different hypotheses; Positive Holes (p-holes) emission from rocks due to tectonic stress (Freund and Sornette, 2007; Freund et al., 2009) or Radon gas emanation from seismogenic region during the earthquake preparation period (Pulinets et al., 2003). According to Freund and Sornette (2007), p-holes from the earthquake breeding zones reached up to the lithosphere and further move to atmosphere as a result of more and more p holes from seismic zone. These p-holes push the atmosphere particle to disturb their original position and further propagate to ionosphere to disturb the pathways of radio signals. On the other hand, (Pulinets et al., 2003; Pulinets and Liu, 2004) showed that Radon emanation from earthquake and associated fault lineament is the source of seismo-ionospheric anomalies. Radon during earthquake preparation period rises up to atmosphere and ionosphere to form ionospheric clouds before and during the release of main shock energy.

The main objective of this study is to detect the ionospheric perturbation in the form of enhancement and depletion of the critical frequency of F2 layer before the M5.6 magnitude earthquake in Pakistan. Furthermore, the temporal extension of long term of data (90 days before/after) is studied for f_oF2 anomaly over the epicenter. We considered the positive or negative anomalies by percentage deviations from the normal distribution. Lastly, found out how these deviations changed with the distance between earthquake preparation zone and ionosonde station.

2. Methodology and observations

2.1. Observation data

We retrieve the data of ionospheric critical frequency from two ionosonde stations of Pakistan Space and Upper Atmosphere Research Commission (SUPARCO) (Fig. 4). The data is collected by an instrumental setup via DISS (Digital Ionospheric Sounder System) of Model-DGS-256 and high frequency (HF) pulse sounding system at the two stations (Fig. 1). Furthermore, the hourly values of ionospheric critical frequency (f_oF2) for the month of September 2019 are studied before the earthquake. The vertical profile of the ionospheric information as digital monogram (records, display and transmit vertical) is shown in Fig. 2.

The ionization process in the ionosphere at daytime remains active and similarly the ionization process at night becomes a bit passive, where only F2 layers persists during night time (Gulyaeva, 2011; Adil et al., 2021). This significant feature of ionosphere makes the radio signals to refract to different extent in atmosphere and ionosphere. Moreover, the ionosphere refracts the minor signals as a shield from the spectrum, as shown in Figs. 2 and 3. On the other hand, frequencies below 1.6 MHz propagate to the monitoring station with the process of amplitude modulation (AM) method. Moreover, as frequency modulated beyond 1.6 MHz, echoes first appear on the ionogram from lower E region, followed by the echoes of F1 and F2 regions with a time delay .

2.2. Methodology

In this paper, the hourly f_oF2 data are investigated for possible ionospheric anomalies induced by the M5.6 Pakistan earthquake. The data is trained by the statistical bound method of upper and lower confidence limits for

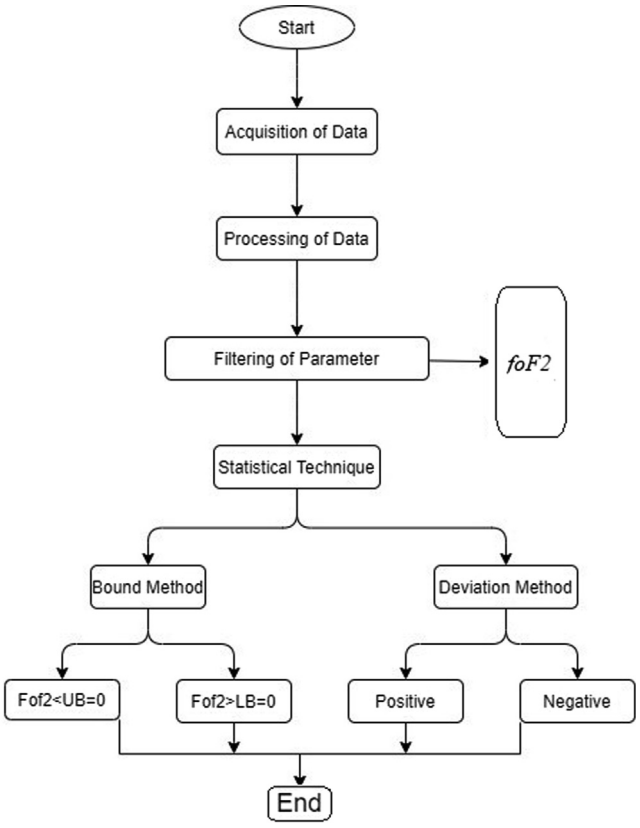

Fig. 1. Flow chart for the preparation and interpretation of ionosonde data (f_oF2).

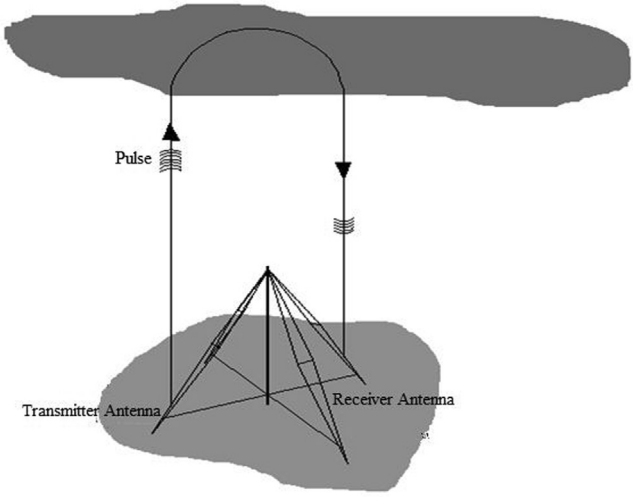

Fig. 2. Ionosonde operation system and its function for retrieving f_oF2 data.

the month of September 2019. This means to detect the irregularity as anomaly before the impending main shock. We calculated the upper (UB) and lower (LB) confidence bounds on the basis of median X and inter quartile range (IQR) from the whole data for September 2019. The bounds are calculated from following equations:

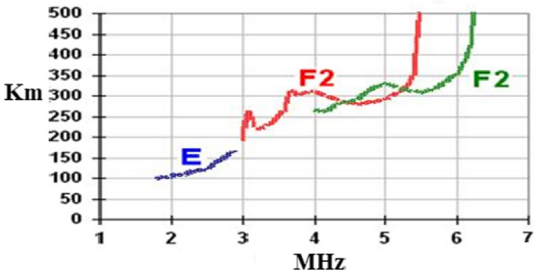

Fig. 3. A daytime ionogram recorded at Islamabad under normal conditions.

$$\text{Upper bound} = X + IQR \quad (1)$$

$$\text{Lower bound} = X - IQR \quad (2)$$

In order to quantify the variations in hourly f_oF2 values, percentage deviation of the time series before the main shock is calculated. The deviation is calculated as the difference between original time series and upper/lower bounds. Percentage deviation is calculated by the equations below:

$$\text{Percent increase in deviations} = \left(\frac{foF2 - UB}{UB}\right) * 100 \quad (3)$$

$$\text{Percent decrease in deviations} = \left(\frac{LB - foF2}{LB}\right) * 100 \quad (4)$$

The positive deviation in percentage for the case of f_oF2 $\leq$ UB is denoted by zero before the earthquake and f_oF2 $\geq$ LB in case of negative deviation is termed as zero percentage. Furthermore, f_oF2 beyond the upper confidence bound is positive anomaly and f_oF2 below lower confidence bound is negative anomaly. The complete process for the execution of seismo-ionospheric anomalies can be seen in the workflow (Fig. 1).

2.3. Case studies

In this paper, seismo-ionospheric anomalies are investigated in daily f_oF2 values before the Mirpur region in Pakistan as precursory signatures. The earthquake and station information are summarized in Table 1. The results of the ionospheric index (f_oF2) in the form of enhancement and depletion in the critical frequency of F2 layer are investigated in the context of Pakistan earthquake. Earthquake information is obtained from United States Geological Survey (USGS) via the web portal (https://earthquake.usgs.gov/earthquakes). This earthquake occurred on September 24, 2019 in Mirpur region, Pakistan, as a result of reverse faulting convergent between the Indian and Eurasian plates. This earthquake hits the region on 11:01 UTC at a shallow hypocentral depth of 10 km. Moreover, this earthquake caused several deaths and huge damages to the infrastructure in the epicentral zone. For the monitoring of seismo-ionospheric anomalies, we analyzed f_oF2

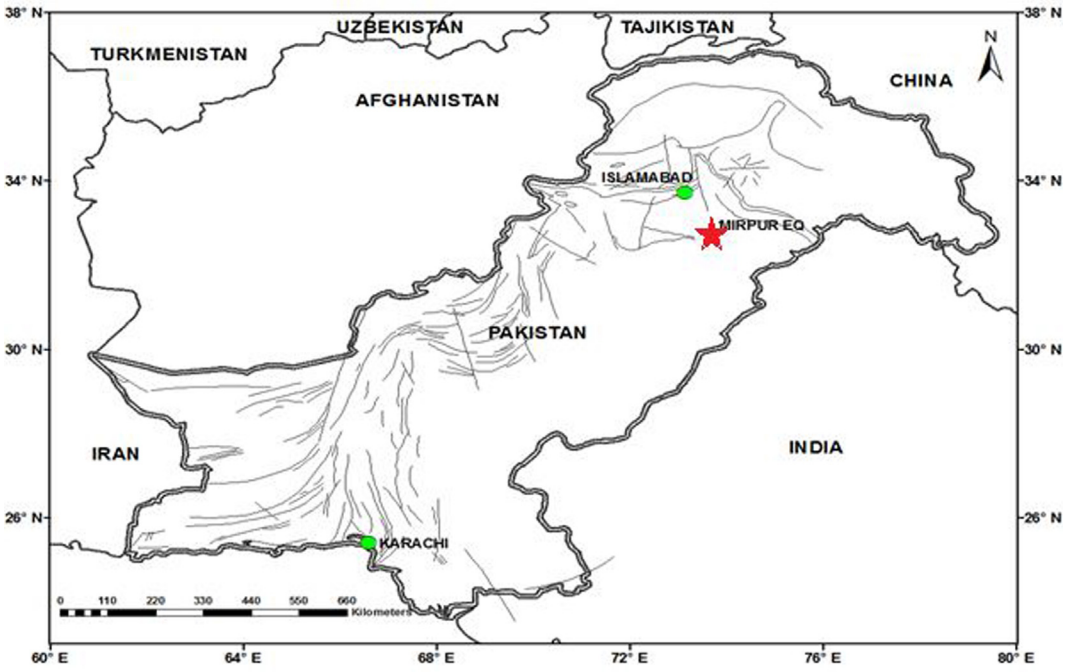

Fig. 4. The geographical locations of the epicenter of the September 24, 2019 (Mw5.6) earthquake and recording ionosonde stations in Pakistan. Epicenter is marked by red star while stations are presented by green circles. (For interpretation of the references to color in this figure legend, the reader is referred to the web version of this article.)

Table 1
Earthquake information w.r.t. Ionosonde stations at Sonmiani and Islamabad.

Date	Time (UT)	Magnitude (M_w)	Depth (km)	Latitude (°N)	Longitude (°E)	Epicentral distance (km) (Sonmiani)	(Islamabad)
24-09-2019	11:01	5.6	10	33.106	73.766	1444	140

data within the seismogenic zone estimated from Dobrovolsky et al. (1979) formula. The epicentral region is calculated from below formula.

$$R = 10^{0.43M}(km) \quad (6)$$

where R and M are the radius of the earthquake preparation zone and magnitude of earthquake, respectively. The seismogenic zone from Dobrovolsky formula depends on the earthquake magnitude: e.g., the larger the magnitude, the large is the earthquake preparation zone and vice versa (Shah et al., 2019a; Abbasi et al., 2020; Kiyani et al., 2020). Moreover, the stations within the earthquake preparation zone and outside the zone are selected to detect seismo-ionospheric anomalies.

The main source of triggering ionospheric anomalies at different altitudes is the geomagnetic storms of medium to high intensity which are due to abnormal solar flares (Mehmood et al., 2021). Furthermore, the geomagnetic storms also cause enhancement and depletion (as seen as ionospheric anomalies) in the critical frequency of F2 layer (Yu et al., 2009). To discriminate the earthquake and geomagnetic storm anomalies, we analyzed the geomagnetic storm data from Omni Web NASA (https://omniweb.gsfc.nasa.gov/cgi/nx1.cgi). Additionally, the geomagnetic indices of K_p and D_{st} index for September 2019 are analyzed to detect storm time ionospheric perturbations in f_oF2, which also executes the spikes in ionosphere at specific intervals.

3. Results and Analysis

The analyses of different results from the two Pakistani f_oF2 stations prior and after the M_w 5.6 Mirpur earthquake have been discussed in detail. The deviation in hourly f_oF2 before and after the earthquake is interpreted on the basis of bounds technique of mean and IQR. Furthermore, the anomalous day values of f_oF2 in percentage deviation are more than 10% or 1/3 of normal f_oF2 distribution beyond the upper and lower confidence limits. Moreover, the abnormal values occur before the main shock during the earthquake preparation period under the hypothesis of lithosphere-ionosphere coupling. Summary of positive and negative earthquakes anomalies from the data of f_oF2 is listed in Table 2.

Table 2
List of the location of ionospheric stations along with details of anomalies before and after the occurrence of a seismic event.

List of Stations	Latitude	Longitude	Precursors observed before event	Precursors observed after event	Observed Anomalies P-positive N-Negative
Sonmiani	25.38°N	66.76°E	10, 8	No	P-10, P-8
Islamabad	33.68°N	73.04°E	10, 9, 8, 5	No	P-10, N-10, P-9, N-9, P-8, P-5

3.1. The Sonmiani station

The Sonmiani Station is located 80 km from Karachi, which is the major city of Pakistan. According to the time series analysis, low ranked ionospheric anomalies are clear in f_oF2 prior to the impending earthquake (Fig. 5). The daily f_oF2 and percent deviation confirm the existence of 10–15% deviation during quiet geomagnetic storm days within 10–15 before the M5.6 earthquake during the analysis of 90 days before/after data. It is also noteworthy to demonstrate the distance between the ionosonde operating station and epicenter for the reality of these low ranked anomalies. The anomalies are more likely less in magnitude due to location difference of earthquake and the station (~13° longitude, which is 1444 km from the Mirpur earthquake location). It shows that the peak plasma density at this station is very far from the earthquake preparation zone, thus no evidence of seismo-ionospheric coupling. On the other hand, low intensity solar storm ($K_p > 3$) also induced no significant anomalies in the peak plasma frequency and some low intensity anomalies occur after the storm days. The high rank f_oF2 anomalies during September 6–11, 2019 have possible relation with the earthquake, as we mainly focused on seismo-ionospheric anomalies within 5–20 days before the main shock. Moreover, the geomagnetic storm intensity is unsettled as per definition of Ulukavak and Inyurt (2019) to generate such long term of anomalies. It is clear in previous reports that the occurrence probability of ionospheric anomaly decreases with the distance from the ionosonde station (Liu et al., 2006; Shah and Jin, 2018; Ahmed et al., 2018). These reports showed that the seismic anomalies were clear at nearby operating stations even in presence of low class ($K_p < 3.5$) geomagnetic storm.

3.2. Islamabad station

The Islamabad Station is located at 130 km from the earthquake epicenter in Dobrovolsky region having geographical coordinates of 33.106°N, 73.766°E and geomag-

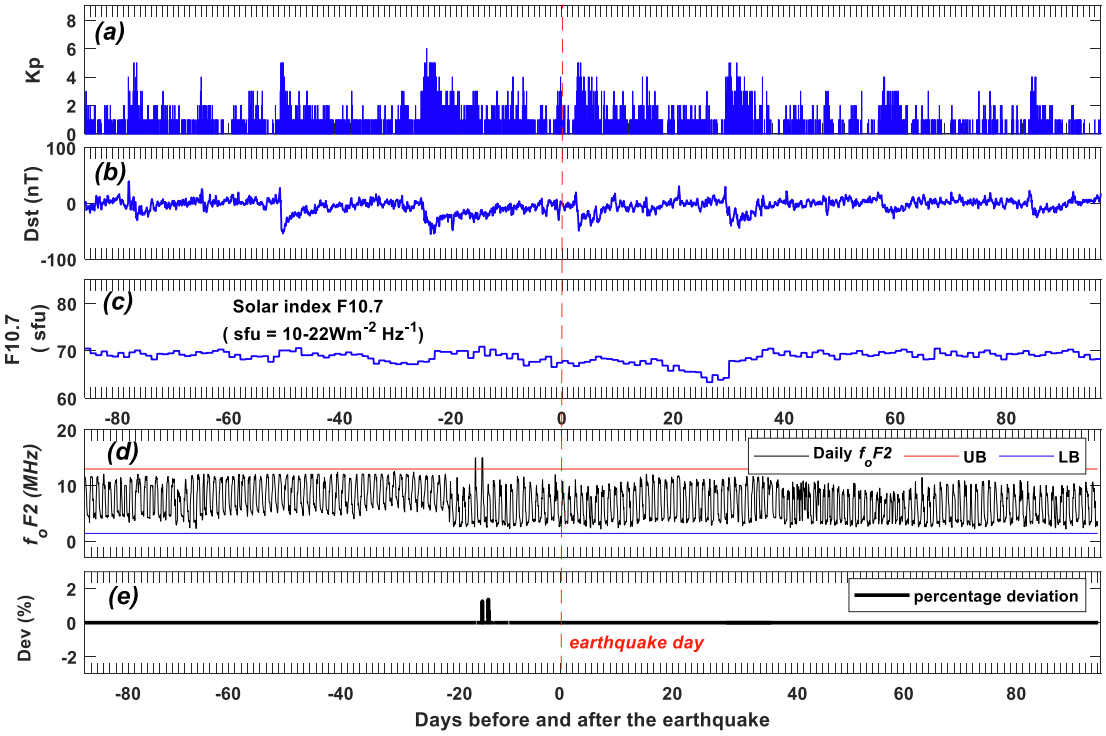

Fig. 5. (a) The figure illustrates the Geomagnetic storm indices for three months before and three months after September 24, 2019 in Kp index, (b) D_{st} values, (c) F10. 7, (d) Variations in the data of f_oF2 obtained at Sonmiani station are shown by black line with their upper and lower bound in red and blue horizontal line, respectively. (e) Percentage deviation in the data of f_oF2. The earthquake day is showed by a red dashed line across all the panels. The day of earthquake occurrence is 24th of September 2019. (For interpretation of the references to color in this figure legend, the reader is referred to the web version of this article.)

netic coordinates of 36.45°N, 79.16°E. Moreover, the distance between the ionosonde station and the epicenter is approximately 140 km (1.26° longitudinal distance). The amplitude of F2 layer critical frequency at the Islamabad station are low in temporal time series within 5–10 before the main shock during the analysis of 90 days before/after data. This anomaly shows synchronization with the epicenter due to its occurrence in quiet geomagnetic storm days. Moreover, a series of higher anomalies occur during 6–12 September and these anomalies may be associated with the impending earthquake. However, it is still not clear due to limited number of stations and low data quality. The location of the station near the epicenter can clue us about impending main shock but more analysis needs to clear the phenomena. There are two reasons for the association of these anomalies with the earthquake under the coupling of lithosphere-ionosphere hypothesis. One is the location of this station within the seismogenic zone (i.e., Dobrovolsky region of the earthquake) and the second is its relation with a series of low intensity ionospheric within 5 days before the earthquake. Furthermore, the observed perturbations within five days before the main shock is <5% in percentage deviation. On the other hand, the deviation of f_oF2 anomalies during 6–12 September is more than 10% from the normal distribution before the Mirpur earthquake. It is clear that the geomagnetic storm intensity ($K_p < 3$) persists from 6 September 2019 till the main shock day and one can see no clear perturbations due to storm (see, e.g., Fig. 6). A sequence of three negative and one positive anomaly occurred on 4, 7, 8 and 5 days, respectively before the impending earthquake (Fig. 6). The percentage deviations further show that negative peaks are of low intensity and positive anomalies occur with high intensity during the seismogenic period before the main shock.

4. Discussion

In this paper, ionospheric anomalies are studied from two different ionosonde stations in Pakistan; where one station is near the epicenter and the other is far from epicenter (i.e., located at 1444 km from the epicenter). According to Liu et al. (2006), the probability of occurrence of seismo-ionospheric anomalies in many cases decreases with the distance from main shock epicenter. In correlation to Liu et al. (2006) conclusions about the occurrence probability of seismo-ionospheric anomalies in nearby stations, this study illustrates that Islamabad station (closer to the epicenter) show more deviation in ionospheric parameters than Sonmiani within 10–20 days before the impending earthquake. Particularly, the spikes in the form of positive and negative anomalies remain invisible in Sonmiani station during 5–10 before the earthquake. Using 30-days median on daily f_oF2 for the detection of earthquake induced ionospheric perturbations, a significant and peculiar feature is identified within 10–20 days prior to the earthquake that is more likely due to main shock energy within earthquake preparation period in both the stations. A series of low intensity positive and negative anomalies occur in Islamabad station, which operates within Dobrovolsky region. On the other hand, high intensity f_oF2 spikes occur during 6–12 September 2019 in both ionosonde stations and these are due to the hypothesis of lithosphere ionosphere coupling.

Sonmiani and Islamabad stations both exhibit the same spikes within 6–12 September 2019 and Sonmiani is very far from the epicenter (operates outside Dobrovolsky region), therefore one cannot claim explicitly the reality of these ionospheric anomalies. However, the variations in Islamabad station are clearly due to the main shock. Some previous reports strongly linked the correlation of ionospheric anomalies and geomagnetic storms (Dautermann et al., 2007; Afraimovich et al., 2008; Thomas et al., 2017) and some even opposed earthquake ionospheric anomalies (e.g., Geller, 1997; Rishbeth, 2007). In this paper, the geomagnetic storm is also not quiet in the first few days of September 2019 before the main shock, with $K_p > 3$ showing a moderate deviation. However, geomagnetic storm causes significant perturbations, which can be seen for more than 10 days before and after the main and recovery phases after sudden storm commencement (Afraimovich et al., 2010; Shah et al., 2020c). Moreover, the median and IQR based bounds provide a good interpretation for seismo-ionospheric anomalies in f_oF2 data, suggesting a specific time (within 10–20 days before) and place (the station within Dobrovolsky region) for the presence of earthquake anomalies. On the other hand, previous records on ionospheric precursors in Taiwan specifically reported significant negative f_oF2 signatures (e.g., Liu et al., 2001, 2004, 2006) and this paper shows similar negative anomalies within 5–10 days prior to the earthquake in Islamabad station (see, e.g., Fig. 6). Similar negative ionospheric deviations were also presented for large magnitude earthquakes in Japan by Ondoh (2000). In this study for seismo-ionospheric signatures, one out of the two stations show low intensity sequential positive and negative anomalies prior of the earthquake within 5–10 days, which can confirm earthquake anomalies induced by the impending main shock in Islamabad station. Furthermore, the anomalies followed by 5–10 days perturbations retain a significant deviation beyond upper bound by a percentage of 5–10% within 10–20 days during the seismic preparation period.

By comparing the anomalies in f_oF2, it is clear that ionospheric anomalies during 6–12 September 2019 before the period of M5.6 earthquake is the execution of main shock; however, no evidence of post seismic anomalies. It means that earthquake induced anomalies occur within 5–20 days before the main shock due to energy emanation process from the epicenter and associated fault lineaments (Fig. 6). Similarly, positive f_oF2 excursion within 5–20 days occurs more significantly than negative anomalies at Islamabad station before the M5.6 earthquake (Fig. 6). The remaining days have normal as compared to abnormal deviation and only few days (Day 5, 8, 9 and 10) show abnormality as compared

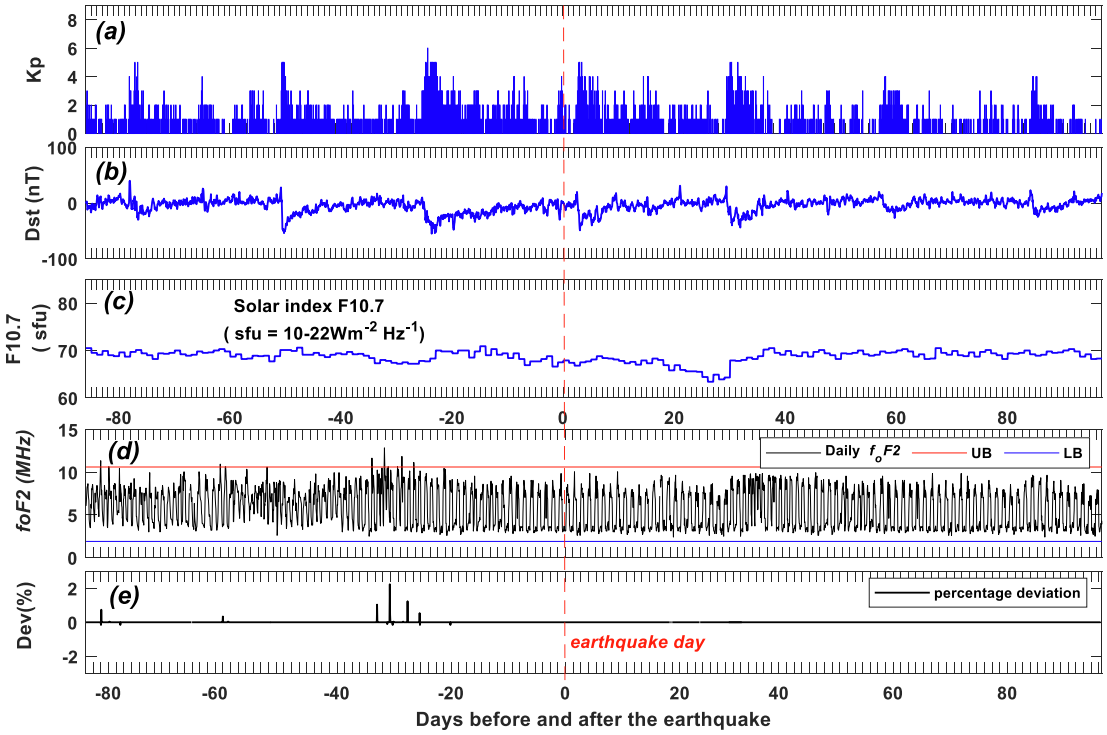

Fig. 6. ΣK_p and Dst indices for three months before and three months after the September 24, 2019 earthquake in panels (a) and (b), respectively. (c) F10.7 analyses in the context of earthquake. (d) the red and blue bars are the upper and lower bounds for hourly data of f_oF2 in black from Islamabad station for two months before and two months after the earthquake occurrence month. (e) The last graph shows the percentage deviation with the black color line. The seismic event of 24th of September 2019 is showed by a red dashed line. (For interpretation of the references to color in this figure legend, the reader is referred to the web version of this article.)

to normal distribution before the earthquake occurrence day. On the other hand, the anomalies in far operating Sonmiani station are all executed by the earthquake during 10–20 days before the main shock. Previous researches have also reported ionospheric anomalies in frequency of E-layer as a precursor (e.g., Ondoh, 2004; Ondoh and Hayakawa, 2006), in some cases earthquake induced f_oF2 perturbations (Ondoh, 2000; Perrone et al., 2010) and some statistical analysis on f_oF2 earthquake anomalies (Liu et al., 2000). Perrone et al. (2010) analyzed ionospheric anomalies related with 10 earthquakes in Italy in the data of Es layer of height h'Es, the perturbations in peak plasma frequency of enclosed Es layer fbEs and similarly foF2 layer. On the other hand, several studies reported the day-to-day variability of ionosphere and particularly emphasized on the ionospheric anomalies due to solar winds, and this variation occurs in our study too (e.g., Danilov, 2013; Popov et al., 2004; Rishbeth et al., 2009). The earthquake induced ionospheric anomalies are the emerging topic of many research studies and sources of seismo-ionospheric anomalies are still controversial. Additionally, very few seismo-ionospheric precursor studies have realized that the thermosphere contributions can also cause variant to the ionosphere (e.g., Pulinets and Liu, 2004; Perrone et al., 2010). Hence, in order to fully predict the earthquake induced ionospheric precursors, more analyses are needed with significantly large satellite observations to measure the variation in lithosphere-ionosphere coupling.

5. Conclusions

We study the ionospheric anomalies from hourly f_oF2 data of Islamabad and Sonmiani station in the context of M5.6 Pakistan earthquake by utilizing the bound method of median and IQR in September 2019. It is noteworthy that Islamabad station operates within the seismogenic zone and another station (i.e., Sonmiani) is operating outside the seismic breeding zone. Evidence shows that high intensity ionospheric peaks occur due to earthquake in both the stations, followed by low intensity positive and negative anomalies only in Islamabad station related to M5.6 earthquakes. The main outcomes of our findings are summarized as follows:

1. A series of high intensity f_oF2 anomalies are recorded during 6–12 September before the earthquake in both ionosonde stations; however, a storm of $K_p > 3$ on 1–2 September induced these anomalies and it is far from the earthquake preparation period. Therefore, we are not clear about the intrinsic nature of these seismo ionospheric anomalies.
2. Only Islamabad station monitors low intensity sequential positive and negative anomalies within 5–10 days before the main shock, which are followed by high intensity ionospheric anomalies in both the stations. There are two possible reasons of these anomalies under the hypothesis of lithosphere-ionosphere coupling. The

first is the location of Islamabad station with reference to earthquake preparation zone as determined by Dobrovolsky and the second is the occurrence of these anomalies within 5–10 days period in quiet storms days ($K_p < 3$).

3. This paper also shows that earthquake induced ionospheric anomalies occur in low intensity (Deviation < 5%). Furthermore, the location of ionosonde station is very important, i.e., the nearby station has large deviation and far station possesses small deviation. Moreover, the lithosphere-ionosphere coupling needs more analysis with dense ionosonde cluster and other satellite measurements.

Declaration of Competing Interest

The authors declare that they have no known competing financial interests or personal relationships that could have appeared to influence the work reported in this paper.

Acknowledgment

We are thankful to USGS, OMNI web for providing earthquake and geomagnetic storm data, respectively. We are also thankful to the editor and two anonymous reviewers for their valuable comments, that assist in furnishing the initial version.

References

Abbasi, A.R., Shah, M., Ahmed, A., Naqvi, N.A., 2020. Possible ionospheric anomalies associated with the 2009 Mw 6.4 Taiwan earthquake from DEMETER and GNSS TEC. Acta Geod. Geophys. 2020. https://doi.org/10.1007/s40328-020-00325-1.

Adil, M.A., Abbas, A., Ehsan, M., Shah, M., Naqvi, N.A., 2021. Investigation of ionospheric and atmospheric anomalies associated with three Mw > 6.5 EQs in New Zealand. J. Geodynamics 145. https://doi.org/10.1016/j.jog.2021.101841 101841.

Afraimovich, E.L., Astafyeva, E.I., Oinats, A.V., Yasukevich, Y.V., Zhivetiev, I.V., 2008. February. Global electron content: a new conception to track solar activity. Annales Geophysicae 26 (2), 335–344, Copernicus GmbH.

Afraimovich, E.L., Ding, F., Kiryushkin, V.V., Astafyeva, E.I., Jin, S., Sankov, V.A., 2010. TEC response to the 2008 Wenchuan earthquake in comparison with other strong earthquakes. Int. J. f Remote Sensing 31 (13), 3601–3613. https://doi.org/10.1080/01431161003727747.

Akhoondzadeh, M., De Santis, A., Marchetti, D., Piscini, A., Jin, S., 2019. Anomalous seismo-LAI variations potentially associated with the 2017 Mw= 7.3 Sarpol-e Zahab (Iran) earthquake from Swarm satellites, GPS-TEC and climatological data. Adv. Space Res. 64 (1), 143–158. https://doi.org/10.1016/j.asr.2019.03.020.

Ahmed, J., Shah, M., Zafar, W.A., Amin, M.A., Iqbal, T., 2018. Seismoionospheric anomalies associated with earthquakes from the analysis of the ionosonde data. J. Atmos. Solar-Terrestrial Phys. 179, 450–458. https://doi.org/10.1016/j.jastp.2018.10.004.

Marchetti, D., De Santis, A., Shen, X., Campuzano, S.A., Perrone, L., Piscini, A., Huang, J., 2020. Possible Lithosphere-Atmosphere-Ionosphere Coupling effects prior to the 2018 Mw= 7.5 Indonesia earthquake from seismic, atmospheric and ionospheric data. J. Asian Earth Sci. 188, 104097.

Danilov, A.D., 2013. Ionospheric F-region response to geomagnetic disturbances. Adv. Space Res. 52 (3), 343–366. https://doi.org/10.1016/j.asr.2013.04.019.

Dautermann, T., Calais, E., Haase, J., Garrison, J., 2007. Investigation ofionospheric electron content variations before earthquakes in southernCalifornia 2003–2004. J. Geophys. Res. Solid Earth 112. https://doi.org/10.1029/2006JB004447.

Dobrovolsky, I.P., Zubkov, S.I., Miachkin, V.I., 1979. Estimation of the size of earthquake preparation zones. Pure Appl. Geophys. 117 (5), 1025–1044. https://doi.org/10.1007/BF00876083.

Forbes, J.M., Palo, S.E., Zhang, X., 2000. Variability of the ionosphere. J. Atmos. Solar-Terrestrial Phys. 62 (8), 685–693. https://doi.org/10.1016/S1364-6826(00)00029-8.

Freund, F., Sornette, D., 2007. Electro-magnetic earthquake bursts and critical rupture of peroxy bond networks in rocks. Tectonophysics 431 (1-4), 33–47. https://doi.org/10.1016/j.tecto.2006.05.032.

Freund, F.T., Kulahci, I.G., Cyr, G., Ling, J., Winnick, M., Tregloan-Reed, J., Freund, M.M., 2009. Air ionization at rock surfaces and pre-earthquake signals. J. Atmos. Solar-Terrestrial Phys. 71 (17-18), 1824–1834. https://doi.org/10.1016/j.jastp.2009.07.013.

Geller, R.J., 1997. Earthquake prediction: a critical review. Geophys. J. Int. 131 (3), 425–450. https://doi.org/10.1111/j.1365-246X.1997.tb06588.x.

Gulyaeva, T.L., 2011. Storm time behavior of topside scale height inferred from the ionosphere–plasmasphere model driven by the F2 layer peak and GPS-TEC observations. Adv. Space Res. 47 (6), 913–920. https://doi.org/10.1016/j.asr.2010.10.025.

Hajkowicz, L.A., 1991. Auroral electrojet effect on the global occurrence pattern of large scale travelling ionospheric disturbances. Planet. Space Sci. 39 (8), 1189–1196. https://doi.org/10.1016/0032-0633(91)90170-F.

Heki, K., 2011. Ionospheric electron enhancement preceding the 2011 Tohoku-Oki earthquake. Geophys. Res. Lett. 38 (17). https://doi.org/10.1029/2011GL047908.

Kiyani, A., Shah, M., Ahmed, A., Shah, H.H., Hameed, S., Adil, M.A., Naqvi, N.A., 2020. Seismo ionospheric anomalies possibly associated with the 2018 Mw 8.2 Fiji earthquake detected with GNSS TEC. J. Geodyn. 140 (101782). https://doi.org/10.1016/j.jog.2020.101782.

Le, H., Liu, J.Y., Liu, L., 2011. A statistical analysis of ionospheric anomalies before 736 M6. 0+ earthquakes during 2002–2010. J. Geophys. Res.: Space Phys. 116 (A2). https://doi.org/10.1029/2010JA015781.

Liu, J.Y., Chen, Y.I., Chuo, Y.J., Chen, C.S., 2006. A statistical investigation of preearthquake ionospheric anomaly. J. Geophys. Res.: Space Phys. 111 (A5). https://doi.org/10.1029/2005JA011333.

Liu, J.Y., Chen, Y.I., Pulinets, S.A., Tsai, Y.B., Chuo, Y.J., 2000. Seismo-ionospheric signatures prior to M≥ 6.0 Taiwan earthquakes. Geophys. Res. Lett. 27 (19), 3113–3116.

Liu, J.Y., Chen, Y.I., Chuo, Y.J., Tsai, H.F., 2001. Variations of ionospheric total electron content during the Chi-Chi earthquake. Geophys. Res. Lett. 28 (7), 1383–1386. https://doi.org/10.1029/2000GL012511.

Liu, J.Y., Chuo, Y.J., Shan, S.J., Tsai, Y.B., Chen, Y.I., Pulinets, S.A., Yu, S.B., 2004. April. Pre-earthquake ionospheric anomalies registered by continuous GPS TEC measurements. Annales Geophysicae 22 (5), 1585–1593.

Marchetti, D., De Santis, A., D'Arcangelo, S., Poggio, F., Jin, S., Piscini, A., Campuzano, S.A., 2020a. Magnetic field and electron density anomalies from Swarm satellites preceding the major earthquakes of the 2016–2017 Amatrice-Norcia (Central Italy) seismic sequence. Pure Appl. Geophys. 177 (1), 305–319. https://doi.org/10.1007/s00024-019-02138-y.

Marchetti, D., De Santis, A., Shen, X., Campuzano, S.A., Perrone, L., Piscini, A., et al., 2020b. Possible Lithosphere-Atmosphere-Ionosphere Coupling effects prior to the 2018 Mw= 7.5 Indonesia earthquake from seismic, atmospheric and ionospheric data. J. Asian Earth Sci. 188. https://doi.org/10.1016/j.jseaes.2019.104097.

Mehmood, M., Filjar, R., Saleem, S., Shah, M., Ahmed, A., 2021. TEC derived from local GPS network in Pakistan and comparison with IRI-

2016 and IRI-PLAS 2017. Acta Geophys. https://doi.org/10.1007/s11600-021-00538-0.

Mendillo, M., Rishbeth, H., Roble, R.G., Wroten, J., 2002. Modelling F2-layer seasonal trends and day-to-day variability driven by coupling with the lower atmosphere. J. Atmos. Solar-Terrestrial Phys. 64 (18), 1911–1931. https://doi.org/10.1016/S1364-6826(02)00193-1.

Mendillo, M., 2006. Storms in the ionosphere: patterns and processes for total electron content. Rev. Geophys. 44 (4). https://doi.org/10.1029/2005RG000193.

Ondoh, T., 2000. Seismo-ionospheric phenomena. Adv. Space Res. 26 (8), 1267–1272. https://doi.org/10.1016/S0273-1177(99)01215-6.

Ondoh, T., 2004. Anomalous sporadic-E ionization before a great earthquake. Adv. Space Res. 34 (8), 1830–1835. https://doi.org/10.1016/j.asr.2003.05.044.

Ondoh, T., Hayakawa, M., 2006. Synthetic study of precursory phenomena of the M7. 2. Hyogo-ken Nanbuearthquakes. Phys. Chem. Earth, Parts A/B/C 31 (4-9), 378–388. https://doi.org/10.1016/j.pce.2006.02.017.

Perrone, L., Korsunova, L.P. Mikhailov, A.V., 2010, April. Ionospheric precursors for crustal earthquakes in Italy. In: Annales Geophysicae, vol. 28, No. 4, Copernicus GmbH, pp. 941–950.

Popov, K.V., Liperovsky, V.A., Meister, C.V., Biagi, P.F., Liperovskaya, E.V., Silina, A.S., 2004. On ionospheric precursors of earthquakes in scales of 2–3 h. Phys. Chem. Earth 29 (4-9), 529–535. https://doi.org/10.1016/j.pce.2003.10.004.

Pulinets, S.A., Legen'Ka, A.D., Gaivoronskaya, T.V., Depuev, V.K., 2003. Main phenomenological features of ionospheric precursors of strong earthquakes. J. Atmos. Solar-terrestrial Phys. 65 (16-18), 1337–1347. https://doi.org/10.1016/j.jastp.2003.07.011.

Pulinets, S.A., Liu, J.Y., 2004. Ionospheric variability unrelated to solar and geomagnetic activity. Adv. Space Res. 34 (9), 1926–1933. https://doi.org/10.1016/j.asr.2004.06.014.

Rishbeth, H., Mendillo, M., Wroten, J., Roble, R.G., 2009. Day-by-day modelling of the ionospheric F2-layer for year 2002. J. Atmos. Solar-Terrestrial Phys. 71 (8–9), 848–856. https://doi.org/10.1016/j.jastp.2009.03.022.

Rishbeth, H., 2006. F-region links with the lower atmosphere? J. Atmos. Solar-Terrestrial Phys. 68 (35), 469–478. https://doi.org/10.1016/j.jastp.2005.03.017.

Rishbeth, H., Mendillo, M., 2001. Patterns of F2-layer variability. J. Atmos. Solar-Terrestrial Phys. 63 (15), 1661–1680. https://doi.org/10.1016/S1364-6826(01)00036-0.

Rishbeth, H., 2007. Do earthquake precursors really exist? Eos, Trans. Am. Geophys. Union 88 (29), 296. https://doi.org/10.1029/2007EO290008.

Shah, M., Jin, S., 2015. Statistical characteristics of seismo-ionospheric GPS TEC disturbances prior to global Mw≥ 5.0 earthquakes (1998–2014). J. Geodynamics 92, 42–49. https://doi.org/10.1016/j.jog.2015.10.002.

Shah, M., Jin, S., 2018. Pre-seismic ionospheric anomalies of the 2013 Mw= 7.7 Pakistan earthquake from GPS and COSMIC observations. Geodesy Geodyn. https://doi.org/10.1016/j.geog.2017.11.008.

Shah, M., Tariq, M.A., Naqvi, N.A., 2019a. Atmospheric anomalies associated with Mw>6.0 earthquakes in Pakistan and Iran during 2010–2017. J. Atmos. Sol. Terr. Phys. 191, 105056. https://doi.org/10.1016/j.jastp.2019.06.003.

Shah, M., Tariq, M.A., Ahmad, J., Naqvi, N.A., Jin, S., 2019b. Seismo ionospheric anomalies before the 2007 M7.7 Chile earthquake from GPS TEC and DEMETER. J. Geodyn. 127, 42–51. https://doi.org/10.1016/j.jog.2019.05.004.

Shah, M., Calabia, A., Tariq, M.A., Ahmed, J., Ahmed, A., 2020a. Possible ionosphere and atmosphere precursory analysis related to Mw & 6.0 earthquakes in Japan. Remote Sens. Environ. 239, 111620. https://doi.org/10.1016/j.rse.2019.111620.

Shah, M., Inyurt, S., Ehsan, M., Ahmed, A., Shakir, M., Ullah, S., Iqbal, M.S., 2020b. Seimo ionospheric anomalies in Turkey associated with Mw≥ 6.0 earthquakesdetected by GPS TEC and GIM TEC. Adv. Space Res. https://doi.org/10.1016/j.asr.2020.03.005.

Shah, M., Ahmed, A., Ehsan, M., Khan, M., Tariq, M.A., Calabia, A., Rahman, Z.ur., 2020c. Total electron content anomalies associated with earthquakes occurred during 1998–2019. Acta Astronaut. 175, 268–276, https://doi.org/10.1016/j.

Shah, M., Qureshi, R.U., Khan, N.G., Ehsan, M., Yan, J., 2021. Artificial Neural Network based thermal anomalies associated with earthquakes in Pakistan from MODIS LST. J. Atmos. Solar-Terrestrial Phys. 215. https://doi.org/10.1016/j.jastp.2021.105568 105568.

Shahzad, R., Shah, M., Ahmed, A., 2021. (2021), Comparison of VTEC from GPS and IRI-2007, IRI-2012 and IRI-2016 over Sukkur, Pakistan. Astrophys. Space Sci. 366, 42. https://doi.org/10.1007/s10509-021-03947-1.

Thomas, J.N., Huard, J., Masci, F., 2017. A statistical study of global ionospheric map total electron content changes prior to occurrences of M≥ 6.0 earthquakes during 2000–2014. J. Geophys. Res.: SpacePhys. 122 (2), 2151–2161. https://doi.org/10.1002/2016JA023652.

Ulukavak, M., Inyurt, S., 2019. Seismo-ionospheric precursors of strong sequential earthquakesin Nepal Region. Acta Astronautica. https://doi.org/10.1016/j.actaastro.2019.09.033.

Yu, T., Mao, T., Wang, Y., Wang, J., 2009. Study of the ionospheric anomaly before the Wenchuan earthquake. Chinese Sci. Bull. 54 (6), 1080–1086. https://doi.org/10.1007/s11434-008-0587-8.